Structural Study of Optical Resolution. IV-b.** The Crystal Structure of $(+)_{589}$-Oxalatobis(ethylenediamine)cobalt(III) Hydrogen-*d*-tartrate Monohydrate and Its Thermal Behavior

Masahiro KURAMOTO, Yoshihiko KUSHI, and Hayami YONEDA*

Department of Chemistry, Faculty of Science, Hiroshima University, Higashi-senda-machi, Hiroshima 730

(Received May 24, 1978)

The crystal structure of $(+)_{589}$-oxalatobis(ethylenediamine)cobalt(III) hydrogen-*d*-tartrate monohydrate, $(+)_{589}$-[Co(ox)en_2]H-*d*-tart·H_2O, has been determined by three-dimensional X-ray analysis. The red crystals are monoclinic, space group $P2_1$, with two molecules in a unit cell of dimensions $a=8.27(1)$, $b=14.60(1)$, $c=7.02(1)$ Å, and $\beta=104.8(2)°$. The structure was solved by Patterson and Fourier methods, and refined by anisotropic block-diagonal least-squares to a conventional *R*-value of 0.100 for the 1265 independent reflections observed. In the diastereoisomer, the optically active complex cation is locked by the $\{H\text{-}d\text{-tart}\}_\infty$ units of the right-handed spiral chains formed along the b-axis. The TG and DSC measurements have been carried out on both less- and more-soluble diastereoisomers of oxalatobis(ethylenediamine)cobalt(III) hydrogen-*d*-tartrate; the difference of their thermal behavior is discussed.

As parts of our structural studies of optical resolution,[1-6] we reported the structures of several diastereoisomers in crystals containing *d*-tartrate anion (*d*-tart^{2-}; *d*-$C_4H_4O_6^{2-}$)[2-4] as the resolving agent. In these compounds, "face-to-face" close contacts between a triangular face of the octahedral complex cation and the *d*-tart^{2-} anion were found.[2-4] The results seem to support the famous "key and lock" hypothesis of Fischer for the diastereomeric discrimination.[7]

Recently, optical resolutions of several complex cations were effected by using hydrogen-*d*-tartrate (H-*d*-tart$^-$; *d*-$C_4H_5O_6^-$) anion as a resolving agent.[8-12] Among them, a simple one-step resolution which provides both optical isomers of oxalatobis(ethylenediamine)cobalt(III) cation, $[Co(ox)en_2]^+$, in high yield was established.[10]

We thought it would be worthwhile to compare the packing manner of the H-*d*-tart$^-$ anion in the above-mentioned diastereoisomers with those of the *d*-tart^{2-} anion in the previous studies. Thus, three-dimensional X-ray analysis of the less-soluble $(+)_{589}$-[Co(ox)en_2]H-*d*-tart·H_2O has been undertaken.

Besides the single crystals of the less-soluble diastereoisomer, the single crystals of the more-soluble isomer, $(-)_{589}$-[Co(ox)en_2]H-*d*-tart·$2H_2O$, could also be obtained, and the thermal behavior of these two diastereoisomers has been examined.

A preliminary communication of this study has already been published.[1]

Experimental

Preparation of Compound. *(a) $(+)_{589}$-[Co(ox)en_2] H-d-tart·H_2O*: The less-soluble diastereoisomer was prepared by the method of Jordan *et al.*[10] Recrystallization from hot aqueous solution of the diastereoisomer gave red crystals. The crystals have a trapezoidal rod shape. Found: C, 27.40; H, 5.32; N, 12.58%. Calcd for $(+)_{589}$-[Co(ox)en_2]H-*d*-tart·H_2O: C, 27.56; H, 5.30; N, 12.90%. The optical purity of these crystals was also checked by the CD-measurement(a JASCO Model J-40CS spectrophotometer with 1 cm cell. ($\Delta\varepsilon_{520}=+2.70$).

(b) $(-)_{589}$-[Co(ox)en_2]H-d-tart·$2H_2O$: After removal of the precipitated crystals of the $(+)_{589}$-diastereoisomer,[10] the filtrate solution was evaporated for 2—3 days at room temperature. The filtration of the $(+)_{589}$-diastereoisomer was continued. This step was repeated three times. As a result, the red crystals of more-soluble $(-)_{589}$-diastereoisomeric salt dihydrate were separated out. The crystals have an octagonal rod shape. Found: C, 26.65; H, 5.64; N, 12.59%. Calcd for $(-)_{589}$-[Co(ox)en_2]H-*d*-tart·$2H_2O$: C, 26.55; H, 5.57; N, 12.39%. The optical purity of these crystals was also checked by the CD-measurement ($\Delta\varepsilon_{523}=-2.18$).

X-Ray Data Measurement. *(a) The Less-soluble Diastereoisomer*: Weissenberg photographs indicated a monoclinic unit cell with systematic extinctions for $0k0$, $k=2n+1$. Of the two possible space groups, $P2_1$ and $P2_1/m$, the latter was eliminated because of the optical activity of the compound. The unit cell dimensions were determined by the least-squares refinement of the *hk*0, *h*0*l*, and 0*kl* reflection data recorded on Weissenberg photographs. The sodium chloride diffraction lines were superimposed on the films for calibration. The crystal data are as follows: monoclinic, space group $P2_1$, $a=8.27(1)$, $b=14.60(1)$, $c=7.02(1)$ Å, $\beta=104.8(2)°$, $D_m=1.74$ g/cm^3 (by flotation in chloroform-bromoform mixture), $Z=2$, and $D_c=1.76$ g/cm^3.

A crystal 0.80 mm long with a cross-sectional area of (0.40×0.35) mm^2 was selected for obtaining the *hk*0—*hk*5 intensity data with Ni $K\alpha$ radiation, using the multiple-film equi-inclination Weissenberg technique. Another crystal, 0.25 mm long with (0.25×0.38) mm^2 cross-sectional area, was used to obtain the intensity data 0*kl*—2*kl*. The intensities were estimated visually with a calibrated intensity scale. A total of 1318 independent reflections were collected. Among them 1265 reflections were observed ($|F_o|>0$) and used for the structure determination. Lorentz, polarization, and spot-shape corrections were applied in the usual manner; corrections for absorption were not made since the value of linear absorption coefficient, μ(Ni $K\alpha$), was 26.7 cm^{-1}.

(b) The More-soluble Diastereoisomer: The crystal data of the more-soluble diastereoisomer were determined similarly. They are as follows: orthorhombic, space group $P2_12_12$, $a=16.56(1)$, $b=14.14(1)$, $c=7.39(1)$ Å, $D_m=1.72$ g/cm^3, $Z=4$, and $D_c=1.74$ g/cm^3.

Thermogravimetric Analysis(TG). TG data were obtained by using a Rigaku Thermal Analyzer Model 8005. A heating rate of 3 °C/min and a static air atmosphere were employed and 9.36—9.71 mg samples were used in each run.

Differential Scanning Calorimetry(DSC). A Rigaku Differential Scanning Calorimeter(Model-8055Cl) was used to

**Ref. 1 corresponds to "Structural Study of Optical Resolution IV-a."

TABLE 1. FINAL ATOMIC PARAMETERS WITH THEIR e.s.d.'s

Atom	x	y	z
Co	0.5556(2)	0.2500(2)	0.5807(2)
O(X1)	0.462(1)	−0.003(1)	0.689(2)
O(X2)	0.542(1)	0.101(1)	1.033(1)
O(X3)	0.514(1)	0.121(1)	0.530(1)
O(X4)	0.575(1)	0.221(1)	0.846(1)
O(T1)	0.190(2)	0.178(1)	0.838(2)
O(T2)	0.119(2)	0.216(1)	1.111(2)
O(T3)	0.232(1)	−0.002(1)	0.960(2)
O(T4)	−0.125(1)	0.055(1)	0.836(2)
O(T5)	−0.123(2)	−0.118(1)	0.932(2)
O(T6)	0.044(1)	−0.101(1)	1.234(2)
O(W)	0.043(2)	0.026(1)	0.535(2)
N(1)	0.314(2)	0.271(1)	0.537(2)
N(2)	0.791(2)	0.230(1)	0.617(2)
N(3)	0.551(1)	0.274(1)	0.305(2)
N(4)	0.583(1)	0.379(1)	0.656(2)
C(E1)	0.278(2)	0.371(1)	0.545(2)
C(E2)	0.831(2)	0.221(1)	0.428(2)
C(E3)	0.728(2)	0.292(1)	0.296(2)
C(E4)	0.425(2)	0.408(1)	0.711(3)
C(X1)	0.501(2)	0.078(1)	0.679(2)
C(X2)	0.543(2)	0.134(1)	0.874(2)
C(T1)	0.157(2)	0.159(1)	0.992(2)
C(T2)	0.154(2)	0.061(1)	1.064(2)
C(T3)	−0.029(2)	0.030(1)	1.027(2)
C(T4)	−0.033(2)	−0.072(1)	1.068(2)

measure the DSC curves. In order to determine the ΔH values of dissociation of the water of crystallization for both diastereoisomers, the instrument was calibrated using the ΔH values of fusion of pure indium, tin, and lead metals as standards. Weights of samples were 8.03 to 13.1 mg. A heating rate of 10 °C/min was used in each run. The dry nitrogen gas(25 ml/min) was used as a furnace atmosphere.

Determination and Refinement of Crystal Structure

The structure was solved by the heavy-atom method. The position of the cobalt atom was determined from the three-dimensional Patterson map. The subsequent Fourier synthesis revealed the positions of all the non-hydrogen atoms. Refinement employing these atomic positions with isotropic thermal parameters converged to a conventional R factor of 0.132 for the 1265 observed reflections, where the R value is $\Sigma||F_o|-|F_c||/\Sigma|F_o|$.

Hydrogen atom co-ordinates, excluding the water molecule and the glycolic hydroxyl and carboxyl groups of H-*d*-tart anion, were calculated (C–H 1.08, N–H 1.00 Å) assuming tetrahedral angles at carbon and nitrogen atoms. Refinement with anisotropic temperature factors for all the non-hydrogen atoms and with fixed hydrogen atom contributions(the isotropic temperature factor $B=3.0$ Å^2 was used) was continued. After four cycles an R value of 0.100 was obtained and the refinement was terminated. The quantity minimized was $w(|F_o|-k|F_c|)^2$ and Cruickshank's weighting scheme[13] was used, where $w=1/(a+|F_o|+b|F_o|^2)$ with $a=5.80$ and $b=0.037$. The atomic scattering factors from the International Tables[14] were used. The dispersion effects were neglected.

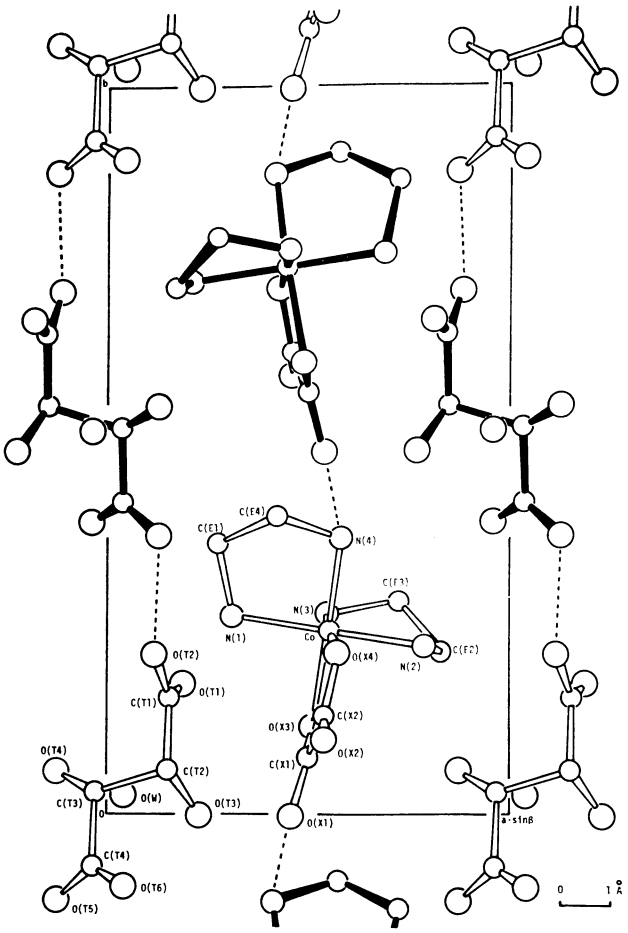

Fig. 1. A perspective drawing of the contents of the unit cell viewed along the c-axis.

All the computations were carried out by a HITAC-8700 computer at the Hiroshima University Computer Center. The computer programs used were FOUR-2/M(Fourier synthesis)[15] and HBLS-IV(Least-squares calculation) with a slight modification.[16]

The final atomic parameters and temperature factors(with their estimated standard deviations) are listed in Tables 1 and 2. Complete lists of the 10-F_o and 10F_c values and the final atomic parameters of the hydrogen atoms have been preserved by the Chemical Society of Japan (Document No. 7838).

Results and Discussion

The crytsal structure consists of discrete $(+)_{589}$-$[Co(ox)en_2]^+$ cations, H-*d*-tart anions, and water molecules. Figures 1 and 2 show the projections of the crystal structure along the c- and b-axis, respectively. Bond distances and angles within the complex cation and the H-*d*-tart anion are listed in Table 3. The water molecules exist around the twofold screw axis at (0, y, 1/2). Each complex cation is surrounded by eight H-*d*-tart anions in a deformed cubic environment.

Cation Geometry. All distances and angles

TABLE 2. ANISOTROPIC TEMPERATURE FACTORS($\times 10^3$) EXPRESSED IN THE FORM $\exp[-2\pi^2(U_{11}h^2a^{*2}+U_{22}k^2b^{*2}+U_{33}l^2c^{*2}+2U_{12}hka^*b^*+2U_{13}hla^*c^*+2U_{23}klb^*c^*)]$.

Atom	U_{11}	U_{22}	U_{33}	U_{12}	U_{13}	U_{23}
Co	40(1)	29(1)	34(1)	−3(1)	4(1)	0(1)
O(X1)	49(6)	13(4)	42(6)	−12(4)	14(5)	−5(4)
O(X2)	52(7)	30(5)	20(5)	−5(5)	11(5)	5(4)
O(X3)	31(5)	29(5)	18(5)	−2(4)	2(4)	0(4)
O(X4)	32(5)	13(4)	22(4)	−8(3)	−3(4)	3(3)
O(T1)	57(7)	27(5)	61(8)	2(5)	29(6)	18(6)
O(T2)	85(9)	16(5)	47(7)	−1(5)	7(7)	4(5)
O(T3)	39(6)	18(5)	59(7)	8(4)	15(5)	−3(5)
O(T4)	29(5)	22(4)	39(6)	4(4)	−2(4)	8(4)
O(T5)	73(9)	17(5)	51(7)	−8(5)	−9(6)	8(5)
O(T6)	41(6)	18(4)	31(5)	−1(4)	6(4)	5(4)
O(W)	76(11)	65(10)	58(9)	4(8)	16(8)	−13(8)
N(1)	34(6)	37(7)	24(6)	−4(5)	0(5)	−6(5)
N(2)	38(6)	14(5)	27(6)	4(4)	0(5)	4(4)
N(3)	24(5)	35(7)	17(5)	−4(4)	0(5)	−1(4)
N(4)	24(5)	27(5)	22(6)	−4(4)	3(5)	−3(5)
C(E1)	28(7)	43(9)	40(9)	2(6)	4(7)	−8(7)
C(E2)	30(7)	33(7)	28(7)	−3(5)	1(6)	0(6)
C(E3)	38(8)	21(6)	26(7)	−3(5)	11(6)	5(5)
C(E4)	41(9)	30(7)	46(10)	5(6)	13(7)	−13(7)
C(X1)	39(7)	20(6)	30(7)	−1(5)	13(6)	−7(5)
C(X2)	35(7)	23(6)	18(7)	−1(5)	5(6)	6(5)
C(T1)	24(7)	29(7)	34(8)	−5(5)	−8(6)	11(6)
C(T2)	30(7)	17(6)	31(7)	4(5)	11(6)	−1(5)
C(T3)	26(7)	18(6)	33(8)	6(5)	13(6)	13(5)
C(T4)	29(7)	23(7)	38(8)	−7(5)	3(6)	0(6)

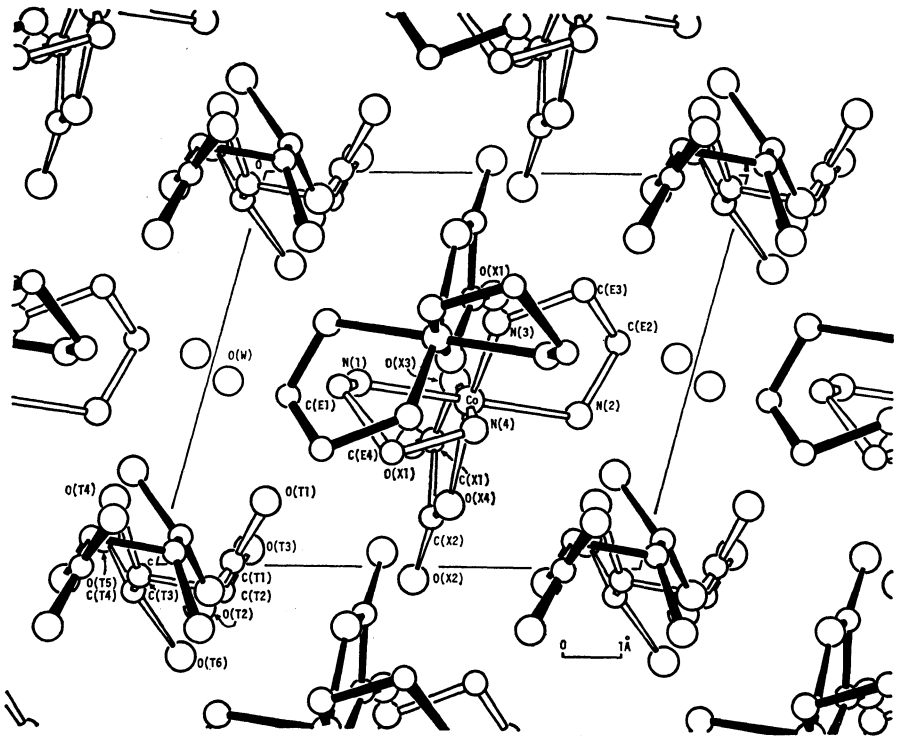

Fig. 2. A projection of the crystal structure along the b-axis.

TABLE 3. BOND DISTANCES AND ANGLES (e.s.d.'s in parentheses)

(a) Bond lengths(Å)

Co-N(1)	1.96(1)	O(X1)-C(X1)	1.23(2)	O(T1)-C(T1)	1.21(2)
Co-N(2)	1.92(1)	O(X2)-C(X2)	1.22(2)	O(T2)-C(T1)	1.29(2)
Co-N(3)	1.96(1)	O(X3)-C(X1)	1.25(2)	O(T3)-C(T2)	1.43(2)
Co-N(4)	1.95(1)	O(X4)-C(X2)	1.32(2)	O(T4)-C(T3)	1.42(2)
Co-O(X3)	1.94(1)	C(E1)-C(E4)	1.55(3)	O(T5)-C(T4)	1.25(2)
Co-O(X4)	1.88(1)	C(E2)-C(E3)	1.50(2)	O(T6)-C(T4)	1.24(2)
N(1)-C(E1)	1.50(2)	C(X1)-C(X2)	1.57(2)	C(T1)-C(T2)	1.52(2)
N(2)-C(E2)	1.46(2)			C(T2)-C(T3)	1.53(2)
N(3)-C(E3)	1.50(2)			C(T3)-C(T4)	1.52(2)
N(4)-C(E4)	1.52(2)				

(b) Bond angles(°)

N(1)-Co-N(4)	86(1)	N(1)-C(E1)-C(E4)	104(1)
N(2)-Co-N(3)	86(1)	N(2)-C(E2)-C(E3)	106(1)
O(X3)-Co-O(X4)	86(0)	N(3)-C(E3)-C(E2)	105(1)
Co-N(1)-C(E1)	111(1)	N(4)-C(E4)-C(E1)	105(1)
Co-N(2)-C(E2)	111(1)	O(X1)-C(X1)-C(X2)	117(1)
Co-N(3)-C(E3)	108(1)	O(X2)-C(X2)-C(X1)	122(1)
Co-N(4)-C(E4)	107(1)	O(X3)-C(X1)-C(X2)	115(1)
Co-O(X3)-C(X1)	113(1)	O(X4)-C(X2)-C(X1)	113(1)
Co-O(X4)-C(X2)	113(1)	O(X1)-C(X1)-O(X3)	128(1)
		O(X2)-C(X2)-O(X4)	125(1)
O(T1)-C(T1)-O(T2)	126(2)	O(T5)-C(T4)-O(T6)	127(1)
O(T1)-C(T1)-C(T2)	122(1)	O(T2)-C(T1)-C(T2)	112(1)
O(T5)-C(T4)-C(T3)	115(1)	O(T6)-C(T4)-C(T3)	118(1)
C(T1)-C(T2)-O(T3)	113(1)	C(T4)-C(T3)-O(T4)	114(1)
O(T3)-C(T2)-C(T3)	106(1)	O(T4)-C(T3)-C(T2)	112(1)

within the complex cation are in good agreement with those in the previous studies.[17,18] The absolute configuration of the complex cation was assigned as *Λ*-$\delta\lambda$ for the $(+)_{589}$-$[Co(ox)en_2]^+$ cation, based on the H-$(+)_{589}$-tartrate anion as an internal reference.[19] Therefore, the geometry of the complex cation is the mirror image of those reported by Aoki *et al.*[17] and Toriumi *et al.*[18]

Recently, it has been reported that, in the $[M(en)_3]^{3+}$ complex cations, the *lel-lel-ob* conformation of three ethylenediamine molecules is the most stable form.[20] Three independent crystal structure analyses are available at present for the $[Co(ox)en_2]^+$ cation, including the present result.[17,18] If these structures were projected down the quasi-threefold axis of the complex cation, a *lel-ob* conformation of the two ethylenediamine molecules was found in every case, though the sizes of the counter anions(Br^-,[17] $(+)_{589}$-$[Co(CN)_2(mal)(NH_3)_2]^-$,[18] and H-*d*-tart$^-$) vary considerably. These results suggest that, in the $[Co(ox)en_2]^+$ cation, the *lel-ob* conformation is the most stable form.

Anion Geometry. The projected sketch of the H-*d*-tart anion is illustrated in Figs. 1 and 2. The O(T1)C(T1)O(T2) group with bond distances C(T1)–O(T1)(1.21 Å) and C(T1)–O(T2)(1.29 Å) and with bond angles O(T1)–C(T1)–C(T2)(122°) and O(T2)–C(T1)–C(T2)(112°) is asymmetric with regard to the C(T1)–C(T2) axis, and obviously this group is considered to be the non-ionized side of the H-*d*-tart anion. In contrast, another O(T5)C(T4)O(T6) group with distances 1.25 and 1.24 Å and with angles 115 and 118° is considered to be the ionized side. These bond distances and angles are in accordance with the previously reported values in H-*d*-tart anions.[19,21-23] Additionally, a short intermolecular distance, O(T2)···O(T5)′ 2.44 Å, was observed. Therefore, the hydrogen atom on the non-symmetrical carboxyl group is possibly bound to O(T2).

The planes including tht five non-hydrogen atoms of each α-hydroxycarboxylate moiety are approximately coplanar. The equations of the least-squares planes are expressed by $-0.840x-0.153y-0.520z+3.464=0$ for the [C(T1), C(T2), O(T1), O(T2), O(T3)] plane and by $0.920x-0.150y-0.361z+4.498=0$ for the [C(T3), C(T4), O(T4), O(T5), O(T6)] plane respectively. The angle between the two planes is slightly less than the corresponding angles of H-*d*-tart anions in other crystals (55.8 *vs.* 62.0,[19] 58.9,[21] 68.7,[22] and 72,1°[23]).

Crystal Packing. In the crystal, H-*d*-tart anions are arranged to make a specific chain structure along the b-axis; they are linked to each other through the hydrogen bonding as shown in Fig. 1. The hydrogen bond distance O(T2)···O(T5) $(-x, 1/2+y, 2-z)$ is 2.44 Å. This hydrogen bond distance is slightly shorter than those of (−)-adrenaline hydrogen-*d*-tartrate,[21] (+)-[(−)-1-methyl-3-benzoylpiperidinium hydrogen-*d*-tartrate]H_2O,[22] and (−)-[(−)-1-methyl-3-ethyl-3-benzoylpiperidinium hydrogen-*d*-tartrate][23] (2.49, 2.63, and 2.49 Å respectively).

Along the b-axis, there is another chain of complex

cations, which are also joined by the hydrogen bond; N(4)···O(X1)($1-x$, $1/2+y$, $1-z$) 2.92 Å. Both chains have the right-handed twofold screw symmetry along the b-axis, as is shown in Fig. 2. Besides, these screw chains are mutually in contact with the following short distances: O(T1)···N(1) 2.91, O(T1)···C(X2) 2.94, O(T1)···O(X2) 3.10, O(T3)···O(X1) 3.01, O(T3)···O(X2) 2.90, O(T4)($1+x$, y, z)···N(2) 2.97, O(T4)($1+x$, y, z)···C(X2) 3.06, O(T4)($1+x$, y, z)···C(X1) 3.02, O(T6)($1-x$, $1/2+y$, $2-z$)···N(2) 2.89, and O(T6)($1-x$, $1/2+y$, $2-z$)···N(4) 3.00 Å.

Table 4. Intermolecular distances($\leq$3.25 Å)

N-H···B	N···B (Å)	H···B (Å)	∠N-H···B
N(1)-H1···O(T1)	2.91[a]	1.91	178
N(1)-H2···O(T2)^{I}	3.12[a]	2.12	171
N(2)-H3···O(T4)^{II}	2.97[a]	1.97	176
N(2)-H4···O(T6)^{III}	2.89[a]	1.92	164
N(3)-H6···O(X2)^{I}	3.17[a]	2.26	150
N(3)-H5···O(X1)^{IV}	3.25[a]	2.50	131
N(4)-H7···O(X1)^{IV}	2.92[a]	1.97	158
N(4)-H8···O(T3)^{III}	3.24	2.45	136
N(4)-H8···O(T6)^{III}	3.00[a]	2.28	128
O(X1)···O(T3)	3.01[a]	—	—
O(X2)···O(T1)	3.10[a]	—	—
O(X2)···O(T3)	2.90[a]	—	—
O(X4)···H14-C(E3)^{V}	3.25	2.41	137
C(X1)···O(T4)^{II}	3.02	—	—
C(X2)···O(T1)	2.94	—	—
C(X2)···O(T4)^{II}	3.06	—	—
O(T2)···O(T5)^{VI}	2.44[a]	—	—
O(W)···O(T1)	3.10	—	—
O(W)···O(T3)	3.03[a]	—	—
O(W)···O(T4)	2.84[a]	—	—
O(W)···O(T6)^{I}	2.81[a]	—	—

Roman numerals as superscripts refer to the following equivalent positions relative to the reference molecule at x, y, z:

I(x, y, $-1+z$), II($1+x$, y, z)
III($1-x$, $1/2+y$, $2-z$), IV($1-x$, $1/2+y$, $1-z$)
V(x, y, $1+z$), VI($-x$, $1/2+y$, $2-z$)

a) Possible hydrogen bonds.

Moreover, along the c-axis, adjacent H-*d*-tart chains are linked by the water molecules with the hydrogen bond distances; O(W)···O(T1) 3.10, O(W)···O(T3) 3.03, O(W)···O(T4) 2.84, and O(W)···O(T6)(x, y, $-1+z$) 2.81 Å. Thus around the water molecule a distorted tetrahedral environment is formed by these four oxygen atoms, and this water molecule has no short contact with the complex cation. Selected intermolecular bond distances and angles are summarized in Table 4.

Difference between d-*Tart*$^{2-}$ *and H-*d*-tart*$^{-}$ *Systems.* Figure 3 shows the arrangement of the $(+)_{589}$-[Co(ox)en_2]$^{+}$ cation and the H-*d*-tart anions projected down the quasi-threefold axis of the complex cation. The adjacent distances between the complex cation and H-*d*-tart anion are: N(1)···O(T2)(x, y, $-1+z$) 3.12, N(2)···O(T6)′($1-x$, $1/2+y$, $2-z$) 2.89, N(4)···O(T6)′($1-x$, $1/2+y$, $2-z$) 3.00, and N(4)···O(T3)′($1-x$, $1/2+y$, $2-z$) 3.24 Å. In this case, there-

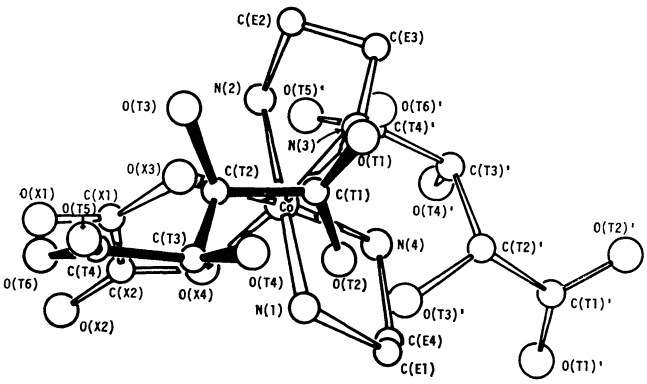

Fig. 3. The arrangement of the complex cation and H-*d*-tart anions projected down the quasi-threefold axis of the complex cation.

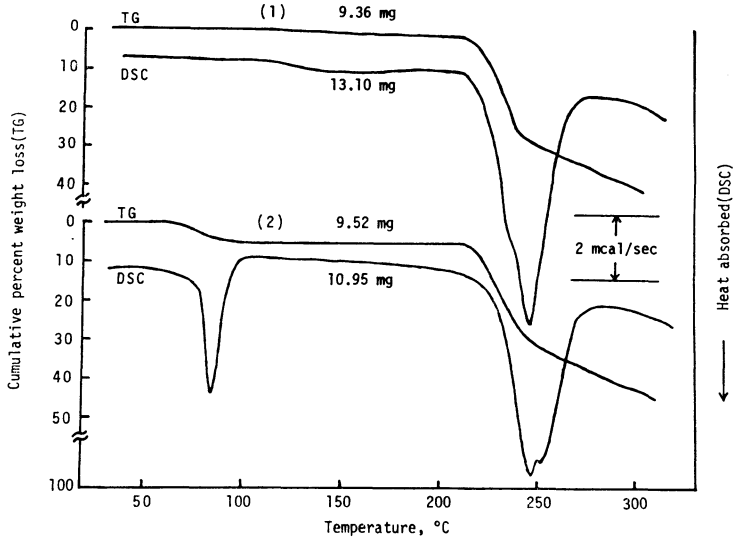

Fig. 4. TG and DSC curves of both diastereoisomers:
(1) $(+)_{589}$-[Co(ox)en_2]H-*d*-tart·H_2O; (2) $(-)_{589}$-[Co(ox)en_2]H-*d*-tart·$2H_2O$.

fore, the characteristic "face-to-face" close contact does not exist between the triangular facet of the octahedral complex cation and the H-*d*-tart anion. Thus, it is suggested that, in the optical resolution process, the discriminative role of the H-*d*-tart anion to the complex cation is quite different from that of the *d*-tartrate anion in the $[M(en)_3]^{3+}\cdots d\text{-tart}^{2-}$ system.[2-4] In other words, in the case of the H-*d*-tart anion, the diastereomeric discrimination is effected even without the "face-to-face" compact fit proposed by Fischer.[7] In the present diastereoisomer the optical-active complex cation, $\Lambda\text{-}\delta\lambda\text{-}(+)_{589}\text{-}[Co(ox)en_2]^+$, is locked by the right-handed spiral chain of $\{H\text{-}d\text{-tart}\}_\infty$ units formed along the b-axis. Then, it seems that the discrimination of optical isomers in this crystal originates in the formation of such a "lock-in-column" mode bonding through the strong hydrogen-bond network.

Thermal Behavior. It is supposed that the thermal behavior of the water of crystallization in both diastereoisomers reflects the difference of the crystal packing modes in these compounds. Therefore, the TG and DSC measurements of both diastereoisomers have been performed. These results are shown in Fig. 4.

The results clearly show that the crystals of the less-soluble diastereoisomer are thermally more stable than those of the more-soluble diastereoisomer. In fact, the water of crystallization is stable up to about 115 °C in the less-soluble salt, the release of the water molecule proceeds very slowly, and no DSC peak is observed. On the other hand, the crystals of the more-soluble salt begin to release the water of crystallization at about 78 °C and the process ceases at 90 °C. The weight loss accompanying this thermal transition is found to be 5.8%. This value is very close to the expected value of the dehydration of $1.5H_2O$(6.0%). A distinct endothermic DSC peak is also observed, as shown in Fig. 4. The ΔH value for the dehydration step is found to be 12.8 kcal/mol(53.6 kJ/mol), which is quite silmilar to those of $(\pm)\text{-}[Co(en)_3]Cl_3\cdot nH_2O$[24] and $(\pm)\text{-}[Cr(en)_3](NCS)_3\cdot H_2O$.[25] Both diastereoisomers are decomposed at about the same temperature(228 °C). Consequently, it is thought that the water of crystallization in the more-soluble salt is more loosely packed crystallographically than that of the less-soluble salt.

Recently, the solubilities of both salts were studied by Shimura and Tsutsui.[26] They mentioned that the solubility of the more-soluble salt, $(-)_{589}\text{-}[Co(ox)en_2]H\text{-}d\text{-tart}\cdot 2.5H_2O$, is three times larger than that of the less-soluble salt, $(+)_{589}\text{-}[Co(ox)en_2]H\text{-}d\text{-tart}\cdot H_2O$, at 25 °C. Moreover, the result of the three-dimensional crystal structure analysis of the more-soluble salt[27] also revealed that the waters of crystallization in this crystal were packed more loosely than those of the less-soluble salt.

We thank the Hiroshima University Computer Center for a generous allocation of computer time and acknowledge a Grant-in-Aid for Scientific Research from the Ministry of Education. We are also grateful to Dr. Kozo Akabori, Hiroshima University, for TG and DSC measurements and for his valuable suggestions.

References

1) M. Kuramoto, Y. Kushi, and H. Yoneda, *Chem. Lett.*, **1976**, 1133.
2) Y. Kushi, M. Kuramoto, and H. Yoneda, *Chem. Lett.*, **1976**, 135.
3) Y. Kushi, M. Kuramoto, and H. Yoneda, *Chem. Lett.*, **1976**, 339.
4) T. Tada, Y. Kushi, and H. Yoneda, *Chem. Lett.*, **1977**, 379.
5) Y. Kushi, M. Kuramoto, and H. Yoneda, *Chem. Lett.*, **1976**, 663.
6) M. Kuramoto, Y. Kushi, and H. Yoneda, *Bull. Chem. Soc. Jpn.*, in press.
7) E. Fischer, *Chem. Ber.*, **32**, 3617 (1899); S. F. Mason, *Ann. Rep.*, **73**, 53 (1976); K. Bernauer, *Topics Current Chem.*, **65**, 1 (1976).
8) J. I. Legg, D. W. Cooke, and B. E. Douglas, *Inorg. Chem.*, **6**, 700 (1967).
9) W. T. Jordan and B. E. Douglas, *Inorg. Chem.*, **12**, 403 (1973).
10) W. T. Jordan, B. J. Brennan, L. R. Froebe, and B. E. Douglas, *Inorg. Chem.*, **12**, 1827 (1973).
11) J. C. Dabrowiak and D. W. Cooke, *Inorg. Chem.*, **14**, 1305 (1975).
12) K. Yamanari, J. Hidaka, and Y. Shimura, *Bull. Chem. Soc. Jpn.*, **50**, 2299 (1977).
13) D. W. J. Cruickshank, "Computing Methods and the Phase Problem in X-Ray Crystal Analysis," ed by R. Pepinsky, J. M. Robertson, and J. C. Speakman, Pergamon Press, Oxford (1961), p. 45.
14) "International Tables for X-Ray Crystallography," Kynoch Press, Birmingham (1968), Vol. III, pp. 201—206.
15) Y. Kushi, unpublished work.
16) T. Ashida, "The Universal Crystallographic Computation Program System," ed by T. Sakurai, The Crystallographic Society of Japan (1967).
17) T. Aoki, K. Matsumoto, S. Ooi, and H. Kuroya, *Bull. Chem. Soc. Jpn.*, **46**, 159 (1973).
18) K. Toriumi, S. Sato, and Y. Saito, *Acta Crystallogr., Sect. B*, **33**, 1378 (1977).
19) A. J. van Bommel and J. M. Bijvoet, *Acta Crystallogr.*, **11**, 61 (1958).
20) R. E. Cramer and J. T. Huneke, *Inorg. Chem.*, **17**, 365 (1978).
21) D. Carlstrøm, *Acta Crystallogr., Sect. B*, **29**, 161 (1973).
22) G. Hite and J. R. Soares, *Acta Crystallogr., Sect. B*, **29**, 2935 (1973).
23) J. R. Ruble, G. Hite, and J. R. Soares, *Acta Crystallogr., Sect. B*, **32**, 136 (1976).
24) H. Chihara and K. Nakatsu, *Bull. Chem. Soc. Jpn.*, **32**, 903 (1956).
25) W. H. Lee and M. F. C. Lord, *Prog. Solid. State Chem.*, **3**, 265 (1967); J. E. House, Jr., and J. C. Bailar, Jr., *J. Inorg. Nucl. Chem.*, **38**, 1791 (1976).
26) Y. Shimura and K. Tsutsui, *Bull. Chem. Soc. Jpn.*, **50**, 145 (1977).
27) M. Kuramoto, Y. Kushi, and H. Yoneda, Presented at the 26th Annual Meeting on Coordination Chemistry of Japan, Sapporo, August 1976, Abstructs 2M04.